

See discussions, stats, and author profiles for this publication at: <https://www.researchgate.net/publication/285542291>

Three-Dimensional Nanoporous Graphene-Carbon Nanotube Hybrid Frameworks for Confinement of SnS₂ Nanosheets: Flexible and Binder-Free Papers with Highly Reversible Lithium Storage

ARTICLE *in* ACS APPLIED MATERIALS & INTERFACES · DECEMBER 2015

Impact Factor: 6.72 · DOI: 10.1021/acsmami.5b09115

READS

15

5 AUTHORS, INCLUDING:



[Yunpeng Huang](#)

Fudan University

38 PUBLICATIONS 321 CITATIONS

[SEE PROFILE](#)



[Wei Fan](#)

Fudan University

28 PUBLICATIONS 425 CITATIONS

[SEE PROFILE](#)



[Tianxi Liu](#)

Fudan University

232 PUBLICATIONS 7,159 CITATIONS

[SEE PROFILE](#)

Article

Three-Dimensional Nanoporous Graphene-Carbon Nanotube Hybrid Frameworks for Confinement of SnS₂ Nanosheets: Flexible and Binder-Free Papers with Highly Reversible Lithium Storage

Longsheng Zhang, Yunpeng Huang, Youfang Zhang, Wei Fan, and Tianxi Liu

ACS Appl. Mater. Interfaces, Just Accepted Manuscript • DOI: 10.1021/acsmami.5b09115 • Publication Date (Web): 01 Dec 2015

Downloaded from <http://pubs.acs.org> on December 8, 2015

Just Accepted

"Just Accepted" manuscripts have been peer-reviewed and accepted for publication. They are posted online prior to technical editing, formatting for publication and author proofing. The American Chemical Society provides "Just Accepted" as a free service to the research community to expedite the dissemination of scientific material as soon as possible after acceptance. "Just Accepted" manuscripts appear in full in PDF format accompanied by an HTML abstract. "Just Accepted" manuscripts have been fully peer reviewed, but should not be considered the official version of record. They are accessible to all readers and citable by the Digital Object Identifier (DOI®). "Just Accepted" is an optional service offered to authors. Therefore, the "Just Accepted" Web site may not include all articles that will be published in the journal. After a manuscript is technically edited and formatted, it will be removed from the "Just Accepted" Web site and published as an ASAP article. Note that technical editing may introduce minor changes to the manuscript text and/or graphics which could affect content, and all legal disclaimers and ethical guidelines that apply to the journal pertain. ACS cannot be held responsible for errors or consequences arising from the use of information contained in these "Just Accepted" manuscripts.



ACS Publications

ACS Applied Materials & Interfaces is published by the American Chemical Society.
1155 Sixteenth Street N.W., Washington, DC 20036

Published by American Chemical Society. Copyright © American Chemical Society.
However, no copyright claim is made to original U.S. Government works, or works
produced by employees of any Commonwealth realm Crown government in the course
of their duties.

1
2
3 **Three-Dimensional Nanoporous Graphene-Carbon Nanotube**
4
5 **Hybrid Frameworks for Confinement of SnS₂ Nanosheets:**
6
7 **Flexible and Binder-Free Papers with Highly Reversible Lithium**
8
9 **Storage**

10
11
12
13
14
15
16 Longsheng Zhang,[†] Yunpeng Huang,[†] Youfang Zhang,[†] Wei Fan,^{*,‡} and Tianxi Liu^{*,†,‡}
17
18
19
20

21 [†]State Key Laboratory of Molecular Engineering of Polymers, Department of
22
23 Macromolecular Science, Fudan University, Shanghai 200433, P. R. China.

24
25 [‡]State Key Laboratory of Modification of Chemical Fibers and Polymer Materials,
26
27 College of Materials Science and Engineering, Donghua University, Shanghai 201620,
28
29 P. R. China.

30
31
32
33
34
35
36 **KEYWORDS:** SnS₂ nanosheets, graphene, carbon nanotubes, confinement, flexible
37
38 anodes, lithium ion batteries

ABSTRACT: The practical applications of transition-metal dichalcogenides for lithium-ion batteries are severely inhibited by their inferior structural stability and electrical conductivity, which can be solved by optimizing these materials to nanostructures and confining them within conductive frameworks. Thus, we report a facile approach to prepare flexible papers with SnS₂ nanosheets (SnS₂ NSs) homogeneously dispersed and confined within the conductive graphene-carbon nanotube (CNT) hybrid frameworks. The confinement of SnS₂ NSs in graphene-CNT matrixes can not only effectively prevent their aggregation during the discharge-charge procedure, but also assist facilitating ion transfer across the interfaces. As a result, the optimized SGC papers gives an improved capacity of 1118.2 mA h g⁻¹ at 0.1 A g⁻¹ along with outstanding stability. This report demonstrates the significance of employing graphene-CNT matrixes for confinement of various active materials to fabricate flexible electrode materials.

1. INTRODUCTION

Nowadays, lithium-ion batteries (LIBs) have been intensively pursued to alleviate the ever-growing demand for efficient energy storage.¹ To fulfill the demands, it has put forward the development of LIBs with higher specific capacity and better cycling life.² Currently, as the most commonly used anode materials for LIBs, the commercialized graphite cannot accommodate the requirement for next-generation LIBs owing to their inferior theoretical capacity.³ Thus, the research for alternative anode materials with higher capacity has received more and more attention.⁴⁻⁸ Recently, a variety of two-dimensional (2D) metal dichalcogenides (e.g. WS₂, SnS₂, etc.) with higher theoretical capacities are studied as potential anodes of the high-power LIBs.⁹⁻¹⁴ Notably, SnS₂ has a sandwiched structure composed of one tier of Sn atom and double tiers of S atoms.¹⁵⁻¹⁷ Additionally, the interlayer spacing between SnS₂ layers is suitable for fast insertion/extraction of lithium ions.¹⁸ Nevertheless, the applications of SnS₂ are held back by their interior structural stability and electrical conductivity.¹⁹⁻²² Besides, it is very hard to reach complete intercalation of restacked SnS₂ nanosheets, thus resulting in reduced electrochemical performance.²³

To address these issues, optimizing the SnS₂ materials to nanostructures and constructing hybrid structures with SnS₂ confined in conductive carbonaceous matrix are effective approaches to accommodate the volumetric expansion and enhance the cyclic stability of SnS₂ nanomaterials.²⁴⁻²⁶ Compared to other carbon nanomaterials, graphene is considered as an ideal matrix to disperse and confine active materials due

to its 2D layered structures, large surface areas and superior electrical conductivity.²⁷⁻²⁹ Nevertheless, the restacking of graphene sheets hampers the utilization of the great potential of graphene.³⁰⁻³¹ Thus, one effective strategy is to incorporate carbon nanotubes (CNTs) between graphene sheets, which will prevent the restacking of graphene.³² With addition of CNTs, the three-dimensional (3D) graphene-CNT composites exhibit greatly enhanced conductivity and surface areas compared with neat graphene.³³⁻³⁴ Nevertheless, the majority of reports about graphene-CNT composites involves addition of cosurfactant that decreases their conductivity,³⁵ or complex approach including chemical vapor deposition.³⁶ Hence, we have reported an effective method to use graphene oxide (GO) to achieve the direct stabilization of pristine CNTs in water *via* mild sonication.³⁷ The incorporated CNTs can greatly deter GO sheets from restacking while GO are able to simultaneously inhibit CNTs from aggregating.³⁸⁻⁴⁰ Moreover, the resulting GO-CNT composites with excellent dispersibility in aqueous solution can be employed to fabricate self-standing papers.⁴¹⁻⁴⁴ More importantly, the flexible graphene-CNT papers possess 3D nanoporous architectures, large specific surface area and interconnected conductive networks, which is expected to be ideal frameworks for immobilization and confinement of electrochemically active materials.⁴⁵⁻⁴⁷

In this work, graphene-CNT composites are utilized as conductive matrixes for immobilization and confinement of ultrathin SnS₂ nanosheets (SnS₂ NSs). Flexible and binder-free graphene-CNT/SnS₂ (SGC) papers have been nicely fabricated by employing GO-CNT composites and SnS₂ NSs *via* a combination of vacuum filtration

and thermal reduction. The SGC papers have porous architectures with ultrathin SnS₂ NSs homogeneously dispersed and confined within the interconnected graphene-CNT matrixes. As a result, the optimized SGC paper gives an enhanced specific capacity (1118.2 mA h g⁻¹) benefiting from cooperative interaction between SnS₂ and graphene-CNT matrixes: (1) unique structures with SnS₂ NSs confined inside the graphene-CNT composites can effectively prevent their aggregation and accommodate their volumetric expansion during the cycling process. (2) The graphene-CNT networks will improve the conductivity of papers by providing conductive networks to facilitate the transportation of charge and lithium ions. (3) The porous structures derived from CNTs and SnS₂ NSs incorporated between the graphene interlayers can enable fast diffusion of Li⁺.

2. EXPERIMENTAL SECTION

2.1. Materials.

Pristine CNTs were purchased from Chengdu Institute of Organic Chemistry. Natural graphite powder and all other reagent were brought by Sinopharm Chemical Reagent Co. Ltd.

2.2. Preparation of SnS₂ nanosheets.

SnS₂ nanosheets (SnS₂ NSs) were prepared through a hydrothermal approach.¹⁵ Typically, 2.5 mmol tin(IV) chloride pentahydrate, 10 mmol thioacetamide and 40 mL water were mixed and then put in 50 mL Teflon autoclave for heating at 160 °C for 12 h. At last, yellow solid was cleaned with water and then dried.

2.3. Preparation of GO-CNT dispersions.

GO sheets was fabricated from graphite through modified Hummers method.⁴⁸ Stable dispersions of GO-CNT composites were synthesized according to our group's approach.³⁷ Briefly, pristine CNTs and dispersions of GO sheets are mixed and sonicated for 2 h. The proportion of GO by weight is two times than CNTs. The unstabilized CNTs are got rid of by further centrifugation and a homogeneous dispersions of GO-CNT composites are fabricated.

2.4. Preparation of Graphene-CNT/SnS₂ papers.

From Figure 1, the flexible Graphene-CNT/SnS₂ (SGC) papers were prepared *via* a facile vacuum filtration and calcination procedure. Typically, a certain amount of SnS₂ NS dispersions and GO-CNT dispersions were mixed by sonicating for 2 h. Then, dispersions of GO-CNT composites and SnS₂ NSs was filtrated *via* a poly(vinylidene fluoride) film filter. In order to reduce GO to graphene, the as-prepared SnS₂/GO-CNT papers were calcined at 350 °C for 3 h under N₂ flow. The SGC papers with GO-CNT composites to SnS₂ mass ratio of 1/2, 2/1 and 1/1 are noted as SGC21, SGC12 and SGC11, respectively. Moreover, graphene-CNT (GC) papers and SnS₂/graphene (SG) papers were prepared by the above process without any SnS₂ or CNT. Correspondingly, the SG papers containing SnS₂ NSs and GO (1/1, w/w) were noted as SG11.

2.5. Materials characterization.

Field emission scanning electron microscopy (FESEM) was conducted on FESEM, Ultra 55. Transmission electron microscopy (TEM) and high-resolution transmission

1
2
3 electron microscopy (HRTEM) were conducted on Tecnai G2 20 TWIN TEM. X-ray
4 diffraction (XRD) pattern was performed with an X’Pert Pro X-ray diffractometer
5 with Cu K_α radiation ($\lambda = 0.1542$ nm) at current of 40 mA and voltage of 40 kV. The
6 Brunauer Emmett Teller (BET) analysis was performed *via* Belsorp-max surface area
7 test instrument by N₂ physisorption at 77 K. X-ray photoelectron spectroscopy (XPS)
8 measurement were investigated by a VG ESCALAB 220I-XL instrument.
9
10
11
12
13
14
15
16
17
18
19

2.6. Electrochemical tests.

20
21 Electrode materials were assembled into coin cells to study their electrochemical
22 performance in an argon-filled glovebox. Celgard-2400 film were employed as
23 separators, lithium foils as counter electrodes and 1 M LiPF₆ in ethylene carbonate
24 (EC)/dimethyl carbonate (DMC)/diethyl carbonate (DEC) (1:1:1, v/v/v) as the
25 electrolytes. The working electrodes were binder-free SGC papers with no conductive
26 additives and binders. In contrast, the SnS₂ NS anodes were fabricated through
27 coating a slurry consisting of conductive carbon-black, SnS₂ NSs and poly(vinylidene
28 fluoride) dispersed in N-methyl-2-pyrrolidinone (8:1:1, w/w/w) on copper foil. Cyclic
29 voltammetry (CV) measurement as well as electrochemical impedance spectroscopy
30 (EIS) were conducted *via* CHI660D workstation (Chenhua Instruments Co. Ltd.).
31
32 Galvanostatic discharge/charge tests and rate capacity at high current densities were
33 investigated through CT2013A device (LAND Electronic Co. Ltd.).
34
35
36
37
38
39
40
41
42
43
44
45
46
47
48
49
50
51
52
53
54

3. RESULTS AND DISCUSSION

3.1. Morphologies and structures.

SEM images in Figure 2a reveals that the lateral size of ultrathin SnS₂ NSs are uniformly from 10 to 30 nm. Corresponding TEM image in Figure 2b also verifies that the SnS₂ NSs are of nanosheet morphologies. More nanostructures of ultrathin SnS₂ NSs obtained from the HRTEM observation (Figure 2c) shows a planar nanosheet with the lattice interlayer of 0.32 nm, related to (100) plane of SnS₂. From HRTEM image of the perpendicular edges of SnS₂ NSs (Figure 2d), the SnS₂ NSs exhibit a typical lamellar structure with about 10 sandwiched S-Sn-S layers and interlayer lattice interlayer of 0.59 nm, which is indexed to (001) plane of SnS₂. From Figure 2e, the size of GO sheets are usually a few micrometers. The AFM analysis of GO sheets (Figure S1) display that GO sheets have a thickness of 1 nm. Due to the hydrophilic groups of the GO sheets (Figure 1), it is readily to form stable dispersions of GO sheets through sonication, which can be employed to achieve direct stabilization of CNTs in water. There is a strong π - π link between GO sheets and CNTs, where the oxygenated group are able to keep the outstanding dispersibility of GO-CNT composites.³⁷ As displayed in Figure 2f, hair-like original CNTs are tightly dispersed onto GO sheets. In the hybrids, GO sheets can greatly deter CNTs from aggregation while the CNTs can hinder GO sheets from restacking at the same time. Notably, both the ultrathin SnS₂ NSs and GO-CNT composites show excellent dispersibility in water (left and middle in Figure S2), and therefore the mixed dispersion of SnS₂ NSs and GO-CNT composites are very stable (right in Figure S2). Excellent dispersibility of SnS₂ NSs and GO-CNT composites in water is crucial for the fabrication of flexible self-standing SGC papers, which is favorable for the

homogeneous dispersion of SnS₂ NSs within the graphene-CNT composites.

From Figure 1, flexible SGC papers are readily prepared *via* facile filtration of a mixed suspension of SnS₂ NSs and GO-CNT composites and subsequent thermal reduction of GO sheets. Figure 3a-3d display the cross-sectional FESEM images of GC, SGC12, SGC11 and SGC21 papers. It can be observed that all papers possess porous sandwiched structures while CNTs incorporated within graphene sheets. Moreover, the content of ultrathin SnS₂ NSs within SGC papers obviously decreases with increased weight ratios of graphene-CNT composites to SnS₂ NSs. As for SGC11 paper (Figure 3c), the SnS₂ NSs confined within the porous graphene-CNT composites can greatly prevent graphene sheets from restacking and deter their pulverization during the discharge-charge procedure. Simultaneously, the well-dispersed SnS₂ NSs are able to provide porous structures and enable swift diffusion of Li⁺. However, excessive amount of SnS₂ NSs in the SGC21 paper will result in severe agglomeration (Figure 3d). The top-view SEM image of SGC11 paper verifies the uniform dispersion of ultrathin SnS₂ NSs within the graphene-CNT matrixes (Figure 3e). Moreover, the EDS mapping analysis also confirm the uniform dispersion of tin, carbon, sulfur and oxygen elements (Figure S3). The low amount of oxygen indicates that the successful reduction of graphene sheets after the calcination procedure.⁴⁹ As displayed in Figure 3f, the average thickness of SGC11 paper is about 6 μm, and it can be tunable by readily varying the amount of the mixed suspensions of SnS₂ NSs and GO-CNT composites for filtration. It is worthy to mention that no breakage is found after bending the flexible SGC11 paper back and forth (inset of

Figure 3f). However, some fractures can be seen with further increased content of SnS₂ NSs in the papers. Thus, the porous structures and good mechanical flexibility of SGC papers are mainly resulted from the cooperative interactions of graphene-CNT composites and SnS₂ NSs.

From the TEM observation in Figure 4a and 4b, SnS₂ NSs and CNTs are uniformly confined within the high-surface-area graphene sheets. The confinement of SnS₂ NSs within GO-CNT hybrid frameworks can effectively prevent them from aggregation and inhibit their volumetric expansion during the cycling process. Figure S4 shows that the graphene sheets in SGC11 paper have 1~2 layers, which are attributed to the ultrathin layered SnS₂ NSs well-dispersed between the graphene layers. In the HRTEM image of SnS₂ NSs in SGC11 paper (Figure 4c), the lattice interlayer of 0.32 nm and 0.27 nm can be indexed to (100) and (101) planes of SnS₂, respectively. The SAED pattern (Figure 4d) reveals the polycrystalline structure of SnS₂ NSs, and the diffuse rings are attributed to (001), (100), (101), (102), (110) and (111) planes of SnS₂, respectively. These results unambiguously confirm the existence of SnS₂ NSs in the SGC papers.

The crystal structures of GO, CNTs, SnS₂ NSs, GO-CNT composites, GC and SGC11 paper were studied using XRD as shown in Figure 5. GO exhibits a diffraction peak at $2\theta = 10.7^\circ$ while CNTs show a diffraction peak at $2\theta = 26.2^\circ$. Two peaks of GO-CNT composites located at $2\theta = 10.7^\circ$ and 26.2° indicate the integration of CNTs with GO sheets. Disappearance of the peak of GC paper located at $2\theta = 10.7^\circ$ confirms the highly reduced graphene sheets. Bare SnS₂ NSs show five diffraction

peaks at $2\theta = 15.3^\circ, 28.8^\circ, 32.5^\circ, 50.4^\circ$ and 52.8° , corresponding to (001), (100), (101), (110) and (111) planes of SnS₂ (JCPDS 23-0667), respectively. The peaks of SGC11 paper suggests the co-existence of GC and SnS₂ NSs. Moreover, the XRD patterns of SGC11, SGC11 and SGC12 papers (Figure S5) all reveal the combination of GC and SnS₂ NSs. Additionally, the intensity of the peaks indexed to SnS₂ all decreases as the proportion of SnS₂ by weight within SGC papers decreases.

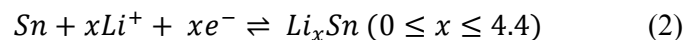
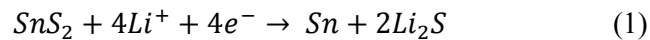
Survey spectrum of SGC11 paper (Figure 6a) confirms the existence of C, Sn, O as well as S elements within SGC11 paper. In high resolution Sn 3d spectrum, the peaks centered at 487.1 eV and 495.6 eV are related with Sn 3d_{5/2} and Sn 3d_{3/2} binding energies (Figure 6b). Notably, S 2p_{1/2} and S 2p_{3/2} orbitals of S²⁻ appear at 162.7 eV and 161.8 eV in the curves of Figure 6c, respectively. These outcomes are in good correspondence with previous literatures about SnS₂.⁵⁰ High resolution C 1s curves of GO-CNT composites and SGC11 paper are displayed in Figure 6d. From the C1s spectra of GO-CNT composites, five peaks located at 284.5, 285.3, 286.8, 287.9 and 288.7 eV are indexed to sp² C, sp³ C, -C-O, -C=O as well as -COO groups, respectively. Contrarily, the intensities of oxygenated carbon peaks of SGC11 paper obviously decrease, indicating the removal of most oxygenated groups of GO sheets.

The BET analysis (Figure 7) indicates SnS₂ NSs as non-porous materials due to its repeatable type II isotherms. The SGC11 and SG11 papers both exhibit IV isotherms, verifying the papers as mesoporous materials. The specific surface area of SnS₂ NSs, SGC11 and SG11 papers are summarized in Table S1. Notably, the specific surface areas of SGC11 and SG11 papers are 148.5 and 96.8 m² g⁻¹, which reveals that the

increased porosity and specific surface area owing to the incorporation of CNTs. Surface area of SGC11 paper is nearly 10 times higher than that ($14.3 \text{ m}^2 \text{ g}^{-1}$) of bare SnS_2 NSs. This is mainly due to the porous architectures derived from graphene-CNT matrixes with open and continuous channels in the papers. Besides, pore size distribution of SGC11 paper is centered at approximately 4 nm (inset of Figure 7), which is in the mesoporous range. The porous structures with higher specific surface area can enable fast diffusion of Li^+ and suppress the volume change of electro-active materials.

3.2. Electrochemical performance.

The electrochemistry of discharge-charge process was investigated by conducting CV tests of SGC11 paper (Figure 8a). During the initial CV cycle, the peaks (1.12 V and 1.68 V) are indexed to transformation of SnS_2 to Sn and Li_2S according to Eq. (1).⁵¹ And the reduction peak (0.30 V) is related with the generation of Li-Sn alloy via a conversion reaction based on Eq. (2). During the anodic process, one peak (0.56 V) is related with delithiation reaction of Li-Sn alloy (Eq. (2)). In the following cycles, the insertion of Li^+ into Sn occurs at 0.9-1.1 V while the decomposition of Li-Sn alloy occurs at 0.4-0.7 V.



In initial lithiation curve of SGC11 papers (Figure 8b), the potential plateaus (1.25 and 1.70 V) are attributed to lithiation of SnS_2 into Sn nanoparticles embedded in Li_2S .

matrix. During the charge process, the potential plateau (0.65 V) is indexed to delithiation procedure of Li-Sn alloy (Eq. (2)). As displayed in Figure 8b, the first discharge-charge specific capacities of SGC11 paper are 1774.3 and 1118.2 mA h g⁻¹, that is 37% for irreversible loss of first cycle. Contrarily, initial charge-discharge capacities of bare SnS₂ NSs are 1434.5 and 556.3 mA h g⁻¹, that is first irreversible loss of 61%. These results reveals the graphene-CNT composites can greatly improve the reversible capacity and reduce the first irreversible loss of SGC paper, which is resulted from the enhanced conductivity as well as the less aggregation and pulverization of SnS₂ NSs in the long-term cycling procedure, therefore decreasing first irreversible loss of SGC papers. Besides, the addition of binders for preparing SnS₂ electrode can also lead to large first irreversible loss. By comparison, the binder-free SGC papers are able to fully utilize the active SnS₂ NSs and conductive graphene-CNT matrixes, thus leading to greatly enhanced specific capacity.

Figure 8c demonstrates the cyclic behaviors of SnS₂ NSs, GC and SGC papers. Neat GC paper manifests 190 mA h g⁻¹ as well as outstanding cyclic behavior while the SnS₂ NS electrode exhibits continuous discharge capacity from 556.3 mA h g⁻¹ to 255.6 mA h g⁻¹ at 50th cycle. Fast decay of SnS₂ NSs is mainly resulted from their bad conductivity, severe aggregation and pulverization after a long cycling process.⁵² In comparison, the SGC12, SGC11 and SGC21 papers deliver improved capacities of 611.3, 1017.5 and 552.4 mA h g⁻¹ at 100th cycle, respectively. Notably, SGC11 paper shows the highest specific capacity owing to the optimized amount of SnS₂ NSs incorporated within graphene-CNT matrixes. Even after the long term cycling

procedure, the SGC11 paper still maintains its original structure with almost unchanged thickness (Figure S6). These results verify that the graphene-CNT matrixes are able to effectively accommodate the large volumetric change of SnS₂ and maintain the structural stability. From Figure S7, the addition of CNTs can improve the conductivity and porosity for fast transportation of ions and lithium ions, thus achieving higher specific capacities of SGC11 papers than SG11 papers.

The rate capabilities of SnS₂ NSs and SGC11 paper (Figure 8d) tells that the SGC11 paper has an enhanced rate performance than bare SnS₂ NSs. Specifically, the reversible capacity of SnS₂ NSs exhibit about 80 mA h g⁻¹ at 2 A g⁻¹, regains 216 mA h g⁻¹ as it reduces to 0.1 A g⁻¹, that is 39% of the original capacity. In contrast, the SGC11 paper exhibits an improved capacity of 634.6 mA h g⁻¹ at 2 A g⁻¹, restores to 972 mAh g⁻¹ as it back to 0.1 A g⁻¹, that is 87% of the original capacity. From Figure S8, SGC11 paper delivers better rate behavior than SGC21 and SGC12 papers. Furthermore, the SGC11 paper exhibits good cyclic stability under high current densities (Figure 9) with its capacity retained at 798.5, 646.2, and 509.1 mA h g⁻¹ at 0.5, 1, and 2 A g⁻¹ at 100th cycle.

The excellent cycling behavior and rate performance of SGC11 paper is ascribed to the cooperative interactions between SnS₂ NSs and graphene-CNT composites. Firstly, the ultrathin SnS₂ NSs are uniformly confined within graphene-CNT matrixes, which can stabilize the structures, deter SnS₂ NSs from aggregation and suppress their volumetric change. Secondly, the graphene-CNT matrixes are able to enhance the conductivity and enable fast transportation of ions. Finally, the porous architectures

derived from SnS₂ NSs well-dispersed within graphene-CNT matrixes are able to facilitate fast diffusion of Li⁺.

To better understand the superior electrochemical performance of SGC papers, EIS tests of SnS₂ NSs, SGC11 and SG11 papers after 10 cycles are present in Figure 10. The Nyquist curves usually have one single semi-circle at high-frequency part as well as one straight line at low-frequency part, indexed to the charge transportation processes and the ion diffusion processes, respectively.⁵³ The radius of semi-circle of SGC11 paper at high-medium frequency part is smaller than that of SnS₂ NSs, indicating its smaller contact and charge-transportation resistance, which directly confirm that the graphene-CNT matrixes can greatly provide fast transportation of Li⁺. Owing to the addition of CNTs, the SGC11 electrode displays smaller semi-circle compared with SG11 electrode, which leads to its improved electrical conductivity and better lithium storage performance.

4. CONCLUSIONS

In summary, flexible self-standing graphene-CNT matrixes with porous structures and excellent electrical conductivity are utilized for immobilization and confinement of SnS₂ nanosheets. The resulting SGC papers with ultrathin SnS₂ NSs homogeneously dispersed and confined within interconnected graphene-CNT matrixes are able to effectively prevent their aggregation and pulverization. Additionally, the conductive graphene-CNT networks are able to greatly improve the conductivity of SGC papers. As a result, the optimized SGC paper exhibits improved performance (1118.2 mA h

¹
²
³ g⁻¹) as well as rate performance with 634.6 mA h g⁻¹ at 2 A g⁻¹. The cooperative
⁴
⁵ interactions between SnS₂ NSs and graphene-CNT matrixes contributes to the
⁶
⁷ enhanced lithium storage performance of SGC papers. Thus, this report highlights the
⁸
⁹ strategy to employ graphene-CNT composites for immobilization and confinement of
¹⁰
¹¹ various active materials to prepare flexible electrodes.
¹²
¹³

¹⁴
¹⁵
¹⁶
¹⁷
¹⁸
¹⁹ **ASSOCIATED CONTENT**
²⁰

²¹ **Supporting Information**
²²

²³ Specific surface area of SnS₂ nanosheets, SGC11 and SG11 papers; AFM analysis of
²⁴
²⁵ graphene oxide; Digital images of suspensions of SnS₂ NSs, GO-CNT composites
²⁶
²⁷ (2/1, w/w) and the mixed suspension of SnS₂ NSs and GO-CNT composites;
²⁸
²⁹ Top-view FESEM image, corresponding EDS spectrum and EDS mapping images of
³⁰
³¹ SGC11 paper; XRD patterns of SGC21, SGC11 and SGC12 papers; Cross-section
³²
³³ FESEM image of SGC11 papers after the cycling test; Cyclic performance of SGC11
³⁴
³⁵ and SG11 papers; Rate performance of SGC21, SGC11 and SGC12 papers at various
³⁶
³⁷ current densities. This information is available free of charge *via* the Internet at
³⁸
³⁹ <http://pubs.acs.org/>.
⁴⁰
⁴¹
⁴²

⁴³
⁴⁴
⁴⁵
⁴⁶
⁴⁷
⁴⁸ **AUTHOR INFORMATION**
⁴⁹

⁵⁰
⁵¹ **Corresponding Author**
⁵²

⁵³ Liu TX* E-mail: txliu@fudan.edu.cn; Tel: +86-21-55664197; Fax: +86-21-65640293.
⁵⁴

⁵⁵ Fan W* E-mail: 12110440003@fudan.edu.cn.
⁵⁶
⁵⁷

Notes

The authors declare no competing financial interest.

ACKNOWLEDGEMENTS

The authors are grateful for the financial support from the National Natural Science Foundation of China (51125011, 51433001).

REFERENCES

- (1) Arico, A. S.; Bruce, P.; Scrosati, B.; Tarascon, J. M.; Van Schalkwijk, W. Nanostructured Materials for Advanced Energy Conversion and Storage Devices. *Nat. Mater.* **2005**, 4, 366-377.
- (2) Cheng, F. Y.; Liang, J.; Tao, Z. L.; Chen, J. Functional Materials for Rechargeable Batteries. *Adv. Mater.* **2011**, 23, 1695-1715.
- (3) Sun, W. W.; Wang, Y. Graphene-Based Nanocomposite Anodes for Lithium-Ion Batteries. *Nanoscale* **2014**, 6, 11528-11552.
- (4) Liang, J.; Yu, X. Y.; Zhou, H.; Wu, H. B.; Ding, S. J.; Lou, X. W. Bowl-Like SnO₂@Carbon Hollow Particles as An Advanced Anode Material for Lithium-Ion Batteries. *Angew. Chem., Int. Ed.* **2014**, 53, 12803-12807.
- (5) Xu, X.; Fan, Z. Y.; Yu, X. Y.; Ding, S. J.; Yu, D. M.; Lou, X. W. A Nanosheets-on-Channel Architecture Constructed from MoS₂ and CMK-3 for High-Capacity and Long-Cycle-Life Lithium Storage. *Adv. Energy Mater.* **2014**, 4, 1400902.

- (6) Gao, G. X.; Lu, S. Y.; Dong, B. T.; Zhang, Z. C.; Zheng, Y. S.; Ding, S. J. One-Pot Synthesis of Carbon Coated Fe₃O₄ Nanosheets with Superior Lithium Storage Capability. *J. Mater. Chem. A* **2015**, 3, 4716-4721.
- (7) Zhu, C. B.; Mu, X. K.; van Aken, P. A.; Maier, J.; Yu, Y. Fast Li Storage in MoS₂-Graphene-Carbon Nanotube Nanocomposites: Advantageous Functional Integration of 0D, 1D, and 2D Nanostructures. *Adv. Energy Mater.* **2015**, 5, 1401170.
- (8) Zhou, X. S.; Yin, Y. X.; Cao, A. M.; Wan, L. J.; Guo, Y. G. Efficient 3D Conducting Networks Built by Graphene Sheets and Carbon Nanoparticles for High-Performance Silicon Anode. *ACS Appl. Mater. Interfaces* **2012**, 4, 2824-2828.
- (9) Huang, X.; Zeng, Z. Y.; Zhang, H. Metal Dichalcogenide Nanosheets: Preparation, Properties and Applications. *Chem. Soc. Rev.* **2013**, 42, 1934-1946.
- (10) Liu, S. Y.; Lu, X.; Xie, J.; Cao, G. S.; Zhu, T. J.; Zhao, X. B. Preferential c-Axis Orientation of Ultrathin SnS₂ Nanoplates on Graphene as High-Performance Anode for Li-Ion Batteries. *ACS Appl. Mater. Interfaces* **2013**, 5, 1588-1595.
- (11) Geng, H.; Kong, S. F.; Wang, Y. NiS Nanorod-Assembled Nanoflowers Grown on Graphene: Morphology Evolution and Li-Ion Storage Applications. *J. Mater. Chem. A* **2014**, 2, 15152-15158.
- (12) Zhang, L. S.; Fan, W.; Liu, T. X. A Flexible Free-Standing Defect-Rich MoS₂/Graphene/Carbon Nanotube Hybrid Paper as A Binder-Free Anode for High-Performance Lithium Ion Batteries. *RSC Adv.* **2015**, 5, 43130-43140.

- (13)Du, Y. C.; Zhu, X. S.; Zhou, X. S.; Hu, L. Y.; Dai, Z. H.; Bao, J. C. Co₃S₄ Porous Nanosheets Embedded in Graphene Sheets as High-Performance Anode Materials for Lithium and Sodium Storage. *J. Mater. Chem. A* **2015**, 3, 6787-6791.
- (14)Du, Y. C.; Zhu, X. S.; Si, L.; Li, Y. F.; Zhou, X. S.; Bao, J. C. Improving the Anode Performance of WS₂ through a Self-Assembled Double Carbon Coating. *J. Phys. Chem. C* **2015**, 119, 15874-15881.
- (15)Zhai, C. X.; Du, N.; Zhang, H.; Yang, D. R. Large-Scale Synthesis of Ultrathin Hexagonal Tin Disulfide Nanosheets with Highly Reversible Lithium Storage. *Chem. Commun.* **2011**, 47, 1270-1272.
- (16)Zhai, C. X.; Du, N.; Zhang, H.; Yu, J. X.; Yang, D. R. Multiwalled Carbon Nanotubes Anchored with SnS₂ Nanosheets as High-Performance Anode Materials of Lithium-Ion Batteries. *ACS Appl. Mater. Interfaces* **2011**, 3, 4067-4074.
- (17)Zhuo, L. H.; Wu, Y. Q.; Wang, L. Y.; Yu, Y. C.; Zhang, X. B.; Zhao, F. Y. One-Step Hydrothermal Synthesis of SnS₂/Graphene Composites as Anode Material for Highly Efficient Rechargeable Lithium Ion Batteries. *RSC Adv.* **2012**, 2, 5084-5087.
- (18)Li, J. P.; Wu, P.; Lou, F. J.; Zhang, P.; Tang, Y. W.; Zhou, Y. M.; Lu, T. H. Mesoporous Carbon Anchored with SnS₂ Nanosheets as An Advanced Anode for Lithium-Ion Batteries. *Electrochim. Acta* **2013**, 111, 862-868.
- (19)Kim, T.; Kirn, C.; Son, D.; Choi, M.; Park, B. Novel SnS₂-Nanosheet Anodes for

- Lithium-Ion Batteries. *J. Power Sources* **2007**, 167, 529-535.
- (20) Ji, L.; Xin, H. L.; Kuykendall, T. R.; Wu, S.; Zheng, H. M.; Rao, M.; Cairns, E. J.; Battaglia, V.; Zhang, Y. G. SnS₂ Nanoparticle Loaded Graphene Nanocomposites for Superior Energy Storage. *Phys. Chem. Chem. Phys.* **2012**, 14, 6981-6986.
- (21) Yin, J. F.; Cao, H. Q.; Zhou, Z. F.; Zhang, J. X.; Qu, M. Z. SnS₂@reduced Graphene Oxide Nanocomposites as Anode Materials with High Capacity for Rechargeable Lithium Ion Batteries. *J. Mater. Chem.* **2012**, 22, 23963-23970.
- (22) Jiang, X.; Yang, X. L.; Zhu, Y.; Shen, J. H.; Fan, K. C.; Li, C. Z. In Situ Assembly of Graphene Sheets-Supported SnS₂ Nanoplates into 3D Macroporous Aerogels for High-Performance Lithium Ion Batteries. *J. Power Sources* **2013**, 237, 178-186.
- (23) Du, N.; Wu, X. L.; Zhai, C. X.; Zhang, H.; Yang, D. R. Large-Scale Synthesis and Application of SnS₂-Graphene Nanocomposites as Anode Materials for Lithium-Ion Batteries with Enhanced Cyclic Performance and Reversible Capacity. *J. Alloys Compd.* **2013**, 580, 457-464.
- (24) Zhang, Q. Q.; Li, R.; Zhang, M. M.; Zhang, B. L.; Gou, X. L. SnS₂/Reduced Graphene Oxide Nanocomposites with Superior Lithium Storage Performance. *Electrochim. Acta* **2014**, 115, 425-433.
- (25) Chen, P.; Su, Y.; Liu, H.; Wang, Y. Interconnected Tin Disulfide Nanosheets Grown on Graphene for Li Ion Storage and Photocatalytic Applications. *ACS Appl. Mater. Interfaces* **2013**, 5, 12073-12082.
- (26) Liu, Z. X.; Deng, H. Q.; Mukherjee, P. P. Evaluating Pristine and Modified SnS₂

as A Lithium-Ion Battery Anode: A First-Principles Study. *ACS Appl. Mater. Interfaces* **2015**, 7, 4000-4009.

(27) Sun, Y. Q.; Wu, Q.; Shi, G. Q. Graphene Based New Energy Materials. *Energy Environ. Sci.* **2011**, 4, 1113-1132.

(28) Tang, C.; Zhang, Q.; Zhao, M. Q.; Tian, G. L.; Wei, F. Resilient Aligned Carbon Nanotube/Graphene Sandwiches for Robust Mechanical Energy Storage. *Nano Energy* **2014**, 7, 161-169.

(29) Fan, W.; Miao, Y. E.; Huang, Y. P.; Tjiu, W. W.; Liu, T. X. Flexible Free-Standing 3D Porous N-Doped Graphene-Carbon Nanotube Hybrid Paper for High-Performance Supercapacitors. *RSC Adv.* **2015**, 5, 9228-9236.

(30) Byon, H. R.; Gallant, B. M.; Lee, S. W.; Shao. Horn, Y. Role of Oxygen Functional Groups in Carbon Nanotube/Graphene Freestanding Electrodes for High Performance Lithium Batteries. *Adv. Funct. Mater.* **2013**, 23, 1037-1045.

(31) Tang, C.; Zhang, Q.; Zhao, M. Q.; Huang, J. Q.; Cheng, X. B.; Tian, G. L.; Peng, H. J.; Wei, F. Nitrogen-Doped Aligned Carbon Nanotube/Graphene Sandwiches: Facile Catalytic Growth on Bifunctional Natural Catalysts and Their Applications as Scaffolds for High-Rate Lithium-Sulfur Batteries. *Adv. Mater.* **2014**, 26, 6100.

(32) Shen, L. F.; Zhang, X. G.; Li, H. S.; Yuan, C. Z.; Cao, G. Z. Design and Tailoring of A Three-Dimensional TiO₂-Graphene-Carbon Nanotube Nanocomposite for Fast Lithium Storage. *J. Phys. Chem. Lett.* **2011**, 2, 3096-3101.

(33) Cheng, Q.; Tang, J.; Ma, J.; Zhang, H.; Shinya, N.; Qin, L. C. Graphene and Carbon Nanotube Composite Electrodes for Supercapacitors with Ultra-High

1
2
3 Energy Density. *Phys. Chem. Chem. Phys.* **2011**, 13, 17615-17624.
4
5

6 (34) Peng, H. J.; Huang, J. Q.; Zhao, M. Q.; Zhang, Q.; Cheng, X. B.; Liu, X. Y.; Qian,
7 W. Z.; Wei, F. Nanoarchitected Graphene/CNT@Porous Carbon with
8 Extraordinary Electrical Conductivity and Interconnected Micro/Mesopores for
9 Lithium-Sulfur Batteries. *Adv. Funct. Mater.* **2014**, 24, 2772-2781.
10
11

12 (35) Hu, Y. H.; Li, X. F.; Wang, J. J.; Li, R. Y.; Sun, X. L. Free-Standing
13 Graphene-Carbon Nanotube Hybrid Papers Used as Current Collector and Binder
14 Free Anodes for Lithium Ion Batteries. *J. Power Sources* **2013**, 237, 41-46.
15
16

17 (36) Park, H. W.; Lee, D. U.; Liu, Y. L.; Wu, J. S.; Nazar, L. F.; Chen, Z. W.
18 Bi-Functional N-Doped CNT/Graphene Composite as Highly Active and Durable
19 Electrocatalyst for Metal Air Battery Applications. *J. Electrochem. Soc.* **2013**,
20 160, 2244-2250.
21
22

23 (37) Zhang, C.; Ren, L. L.; Wang, X. Y.; Liu, T. X. Graphene Oxide-Assisted
24 Dispersion of Pristine Multiwalled Carbon Nanotubes in Aqueous Media. *J. Phys.*
25
26 *Chem. C* **2010**, 114, 11435-11440.
27
28

29 (38) Zhang, C.; Tjiu, W. W.; Liu, T. X. All-Carbon Composite Paper as A Flexible
30 Conducting Substrate for the Direct Growth of Polyaniline Particles and Its
31 Applications in Supercapacitors. *Polym. Chem.* **2013**, 4, 5785-5792.
32
33

34 (39) Yang, S. Y.; Chang, K. H.; Tien, H. W.; Lee, Y. F.; Li, S. M.; Wang, Y. S.; Wang,
35 J. Y.; Ma, C.; Hu, C. C. Design and Tailoring of A Hierarchical
36 Graphene-Carbon Nanotube Architecture for Supercapacitors. *J. Mater. Chem.*
37 **2011**, 21, 2374-2380.
38
39

- (40) Peng, L. W.; Feng, Y. Y.; Lv, P.; Lei, D.; Shen, Y. T.; Li, Y.; Feng, W. Transparent, Conductive, and Flexible Multiwalled Carbon Nanotube/Graphene Hybrid Electrodes with Two Three-Dimensional Microstructures. *J. Phys. Chem. C* **2012**, 116, 4970-4978.
- (41) Lu, X. J.; Dou, H.; Gao, B.; Yuan, C. Z.; Yang, S. D.; Hao, L.; Shen, L. F.; Zhang, X. G. A Flexible Graphene/Multiwalled Carbon Nanotube Film as A High Performance Electrode Material for Supercapacitors. *Electrochim. Acta* **2011**, 56, 5115-5121.
- (42) Cheng, Y. W.; Lu, S. T.; Zhang, H. B.; Varanasi, C. V.; Liu, J. Synergistic Effects from Graphene and Carbon Nanotubes Enable Flexible and Robust Electrodes for High-Performance Supercapacitors. *Nano Lett.* **2012**, 12, 4206-4211.
- (43) Huang, Z. D.; Zhang, B. A.; Oh, S. W.; Zheng, Q. B.; Lin, X. Y.; Yousefi, N.; Kim, J. K. Self-Assembled Reduced Graphene Oxide/Carbon Nanotube Thin Films as Electrodes for Supercapacitors. *J. Mater. Chem.* **2012**, 22, 3591-3599.
- (44) Tan, Y. Q.; Song, Y. H.; Zheng, Q. Facile Regulation of Glutaraldehyde-Modified Graphene Oxide for Preparing Free-Standing Papers and Nanocomposite Films. *Chin. J. Polym. Sci.* **2013**, 31, 399-406.
- (45) Yuan, C. Z.; Yang, L.; Hou, L. R.; Li, J. Y.; Sun, Y. X.; Zhang, X. G.; Shen, L. F.; Lu, X. J.; Xiong, S. L.; Lou, X. W. Flexible Hybrid Paper Made of Monolayer Co₃O₄ Microsphere Arrays on rGO/CNTs and Their Application in Electrochemical Capacitors. *Adv. Funct. Mater.* **2012**, 22, 2560-2566.

- (46) Han, K.; Liu, Z.; Ye, H. Q.; Dai, F. Flexible Self-Standing Graphene-Se@CNT Composite Film as A Binder-Free Cathode for Rechargeable Li-Se Batteries. *J. Power Sources* **2014**, 263, 85-89.
- (47) Huang, J. Q.; Peng, H. J.; Liu, X. Y.; Nie, J. Q.; Cheng, X. B.; Zhang, Q.; Wei, F. Flexible All-Carbon Interlinked Nanoarchitectures as Cathode Scaffolds for High-Rate Lithium-Sulfur Batteries. *J. Mater. Chem. A* **2014**, 2, 10869-10875.
- (48) Hummers, W. S.; Offeman, R. E. Preparation of Graphitic Oxide. *J. Am. Chem. Soc.* **1958**, 80, 1339.
- (49) Lu, J. L.; Liu, W. S.; Ling, H.; Kong, J. H.; Ding, G. Q.; Zhou, D.; Lu, X. H. Layer-by-Layer Assembled Sulfonated-Graphene/Polyaniline Nanocomposite Films: Enhanced Electrical and Ionic Conductivities, and Electrochromic Properties. *RSC Adv.* **2012**, 2, 10537-10543.
- (50) Jiang, Z. F.; Wang, C.; Du, G. H.; Zhong, Y. J.; Jiang, J. Z. In Situ Synthesis of SnS₂@Graphene Nanocomposites for Rechargeable Lithium Batteries. *J. Mater. Chem.* **2012**, 22, 9494-9496.
- (51) Luo, B.; Fang, Y.; Wang, B.; Zhou, J. S.; Song, H. H.; Zhi, L. J. Two Dimensional Graphene-SnS₂ Hybrids with Superior Rate Capability for Lithium Ion Storage. *Energy Environ. Sci.* **2012**, 5, 5226-5230.
- (52) Chang, K.; Wang, Z.; Huang, G. C.; Li, H.; Chen, W. X.; Lee, J. Y. Few-Layer SnS₂/Graphene Hybrid with Exceptional Electrochemical Performance as Lithium-Ion Battery Anode. *J. Power Sources* **2012**, 201, 259-266.
- (53) Kong, J. H.; Yee, W. A.; Yang, L. P.; Wei, Y. F.; Phua, S. L.; Ong, H. G.; Ang, J.

M.; Li, X.; Lu, X. H. Highly Electrically Conductive Layered Carbon Derived from Polydopamine and Its Functions in SnO₂-Based Lithium Ion Battery Anodes.
Chem. Commun. **2012**, 48, 10316-10318.

Figure captions:

Figure 1. Schematic illustration of the preparation procedure of flexible self-standing Graphene-CNT/SnS₂ hybrid paper.

Figure 2. (a) FESEM and (b) TEM images of SnS₂ NSs. HRTEM images of (c) planar and (d) perpendicular SnS₂ NSs. TEM images of (e) GO sheets and (f) GO-CNT composites.

Figure 3. Cross-sectional FESEM images of (a) GC, (b) SGC12, (c) SGC11 and (d) SGC21 papers. (e) Top-view FESEM image of SGC11 paper. (f) Cross-sectional FESEM image of SGC11 paper at low magnification. The inset of (f) shows the digital photo of flexible self-standing SGC11 paper.

Figure 4. (a, b) TEM and (c) HRTEM images of SGC11 paper. (d) SAED pattern of SnS₂ NSs in the SGC11 paper.

Figure 5. XRD patterns of GO, CNT, GO-CNT composites, SnS₂ NSs, GC and SGC11 papers.

Figure 6. (a) XPS survey spectrum, high resolution (b) Sn 3d spectrum and (c) S 2p spectrum of SGC11 paper. (d) C 1s spectra of SGC11 paper and GO-CNT composites.

Figure 7. Nitrogen adsorption isotherms of SnS₂ NSs, SG11 and SGC11 papers. The inset shows the corresponding pore size distribution of the SGC11 paper.

Figure 8. (a) CV curves (1st, 2nd and 5th cycles) of SGC11 paper measured at a scan rate of 0.1 mV s⁻¹. (b) The discharge/charge curves of SGC11 paper in the 1st, 2nd and 5th cycles. (c) Cycling performance of SnS₂ NSs, GC, SGC21, SGC11 and SGC12

1
2
3 papers in the voltage range from 0.01 to 3.0 V at a current density of 0.1 A g⁻¹. (d)
4
5
6 Rate performance of SnS₂ NSs and SGC11 paper at various current densities.
7
8

9 **Figure 9.** High-rate cycling performance of SGC11 paper in the voltage range from
10 0.01 to 3.0 V at a current density of 0.5, 1 and 2 A g⁻¹.
11
12

13 **Figure 10.** Nyquist plots of SnS₂ NSs, SG11 and SGC11 papers measured in the
14 frequency range from 100 kHz to 0.01 Hz with an AC voltage amplitude of 5.0 mV.
15
16
17
18
19
20
21
22
23
24
25
26
27
28
29
30
31
32
33
34
35
36
37
38
39
40
41
42
43
44
45
46
47
48
49
50
51
52
53
54
55
56
57
58
59
60

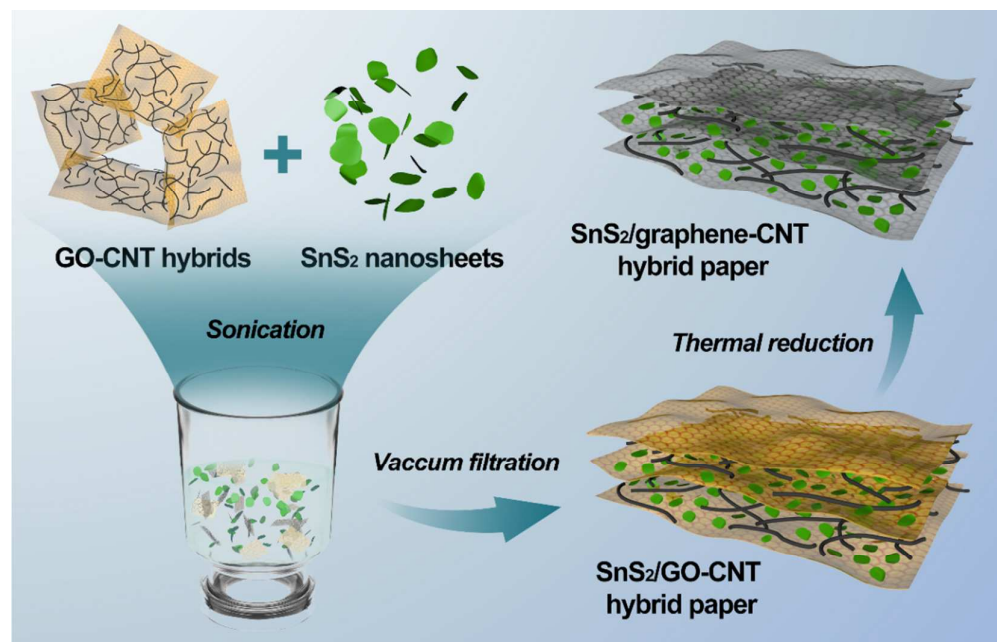


Figure 1

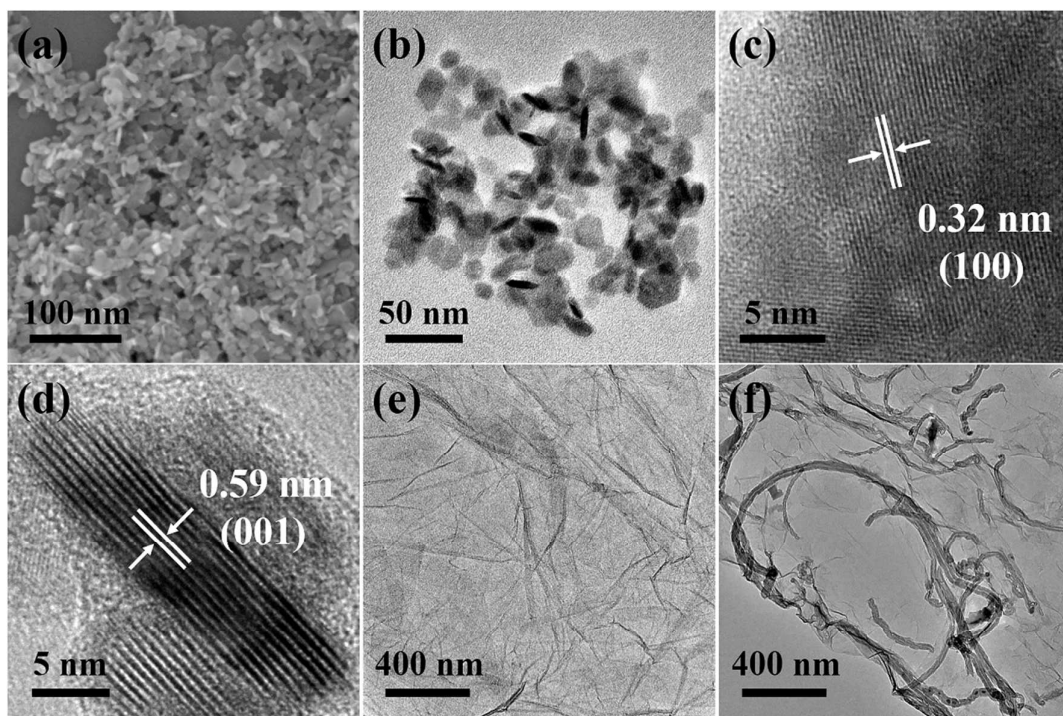


Figure 2

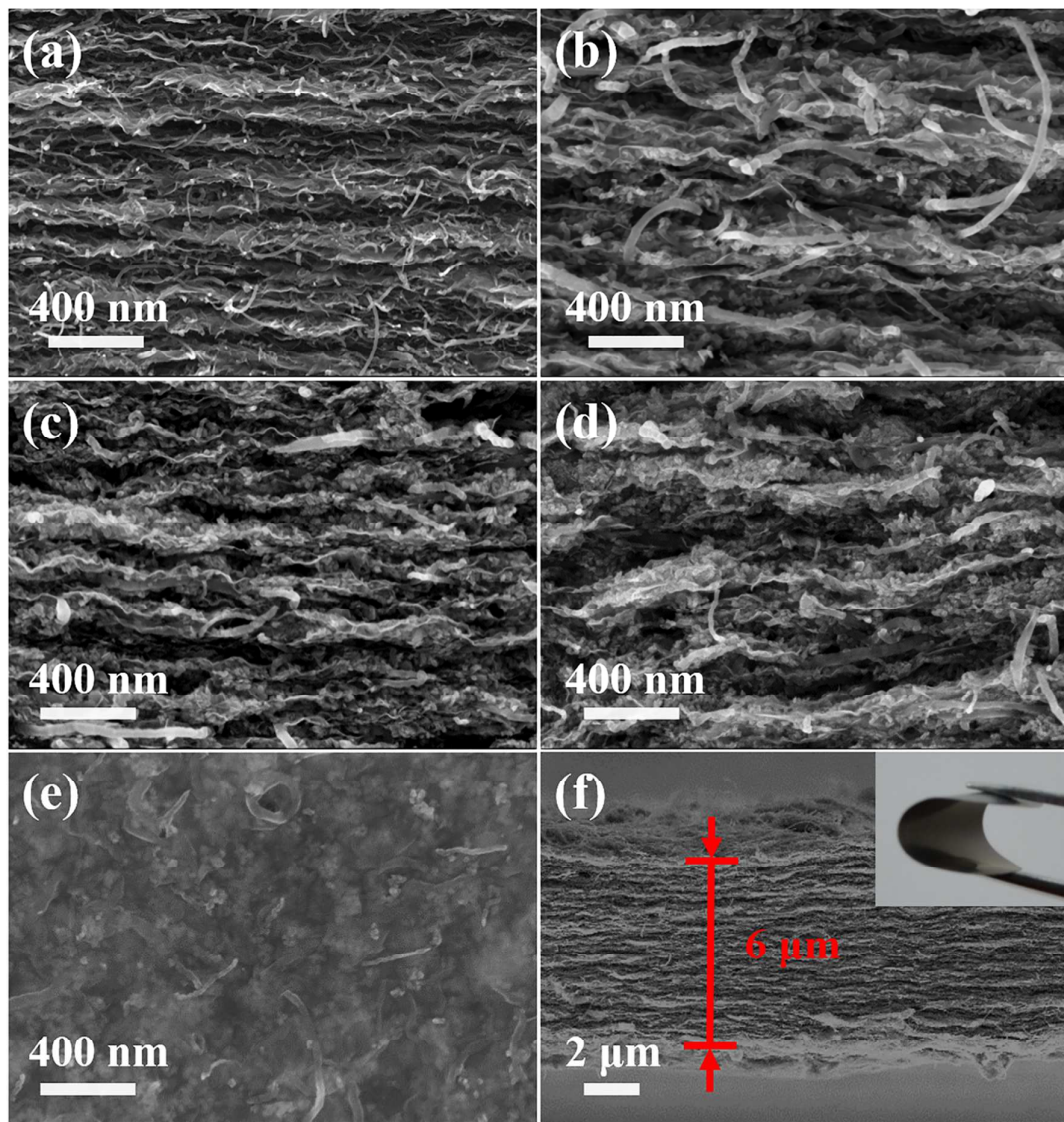


Figure 3

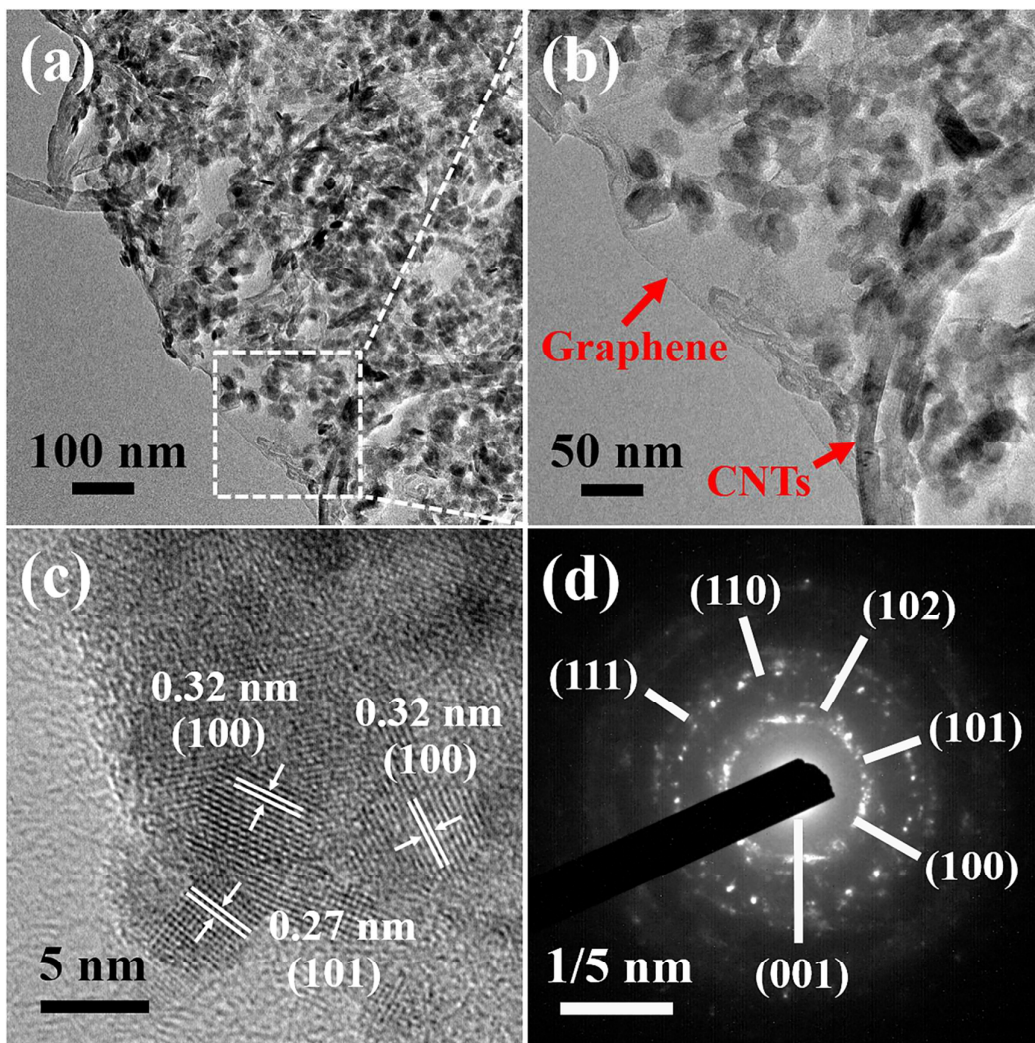


Figure 4

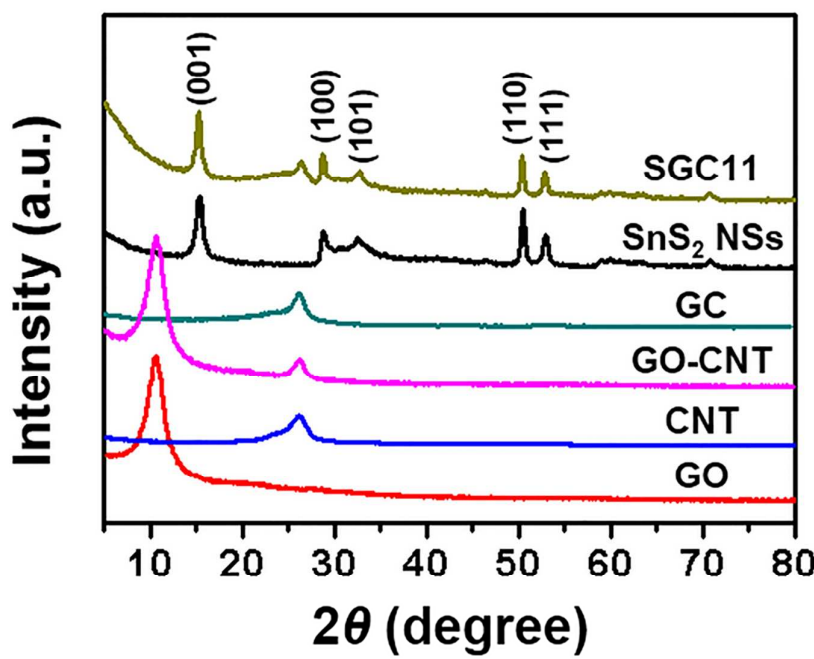


Figure 5

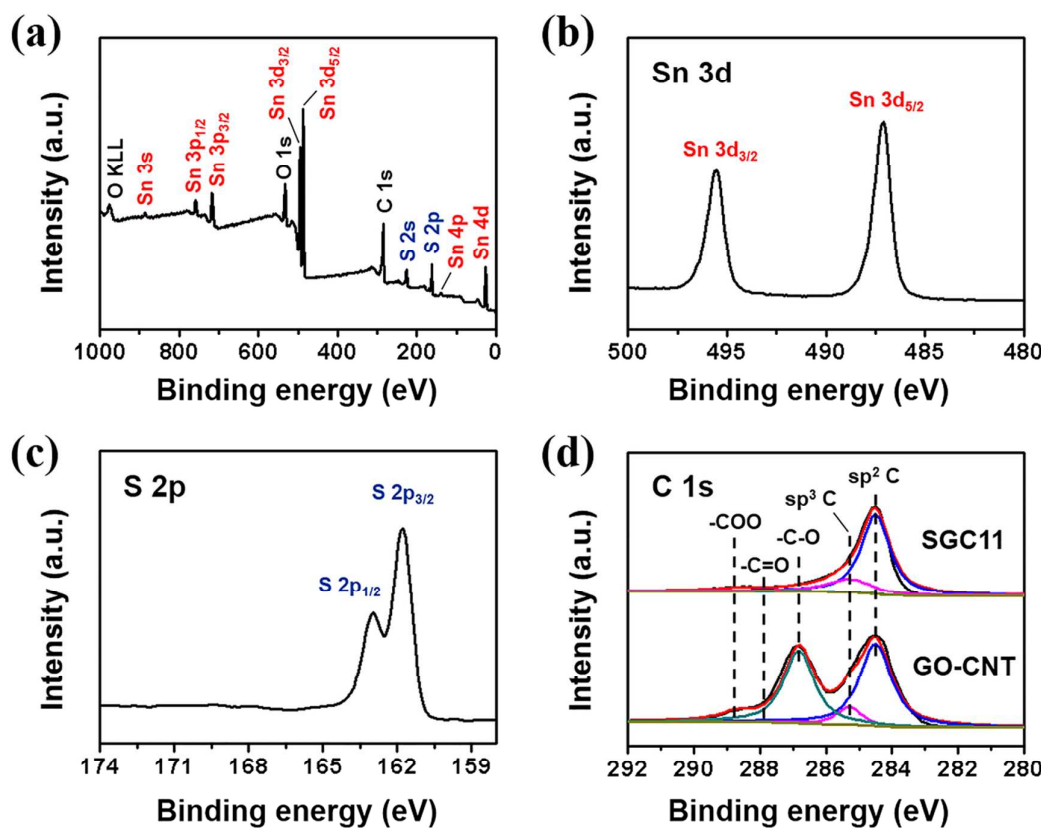


Figure 6

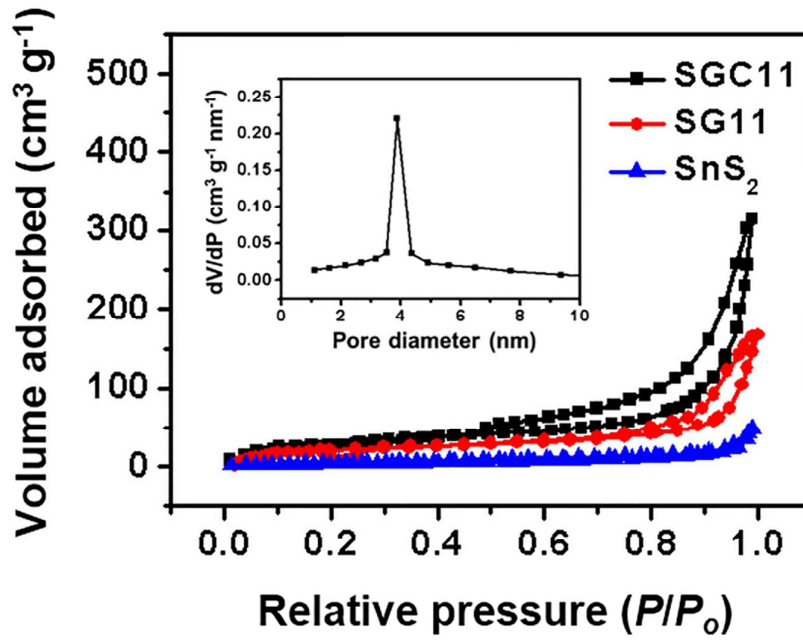


Figure 7

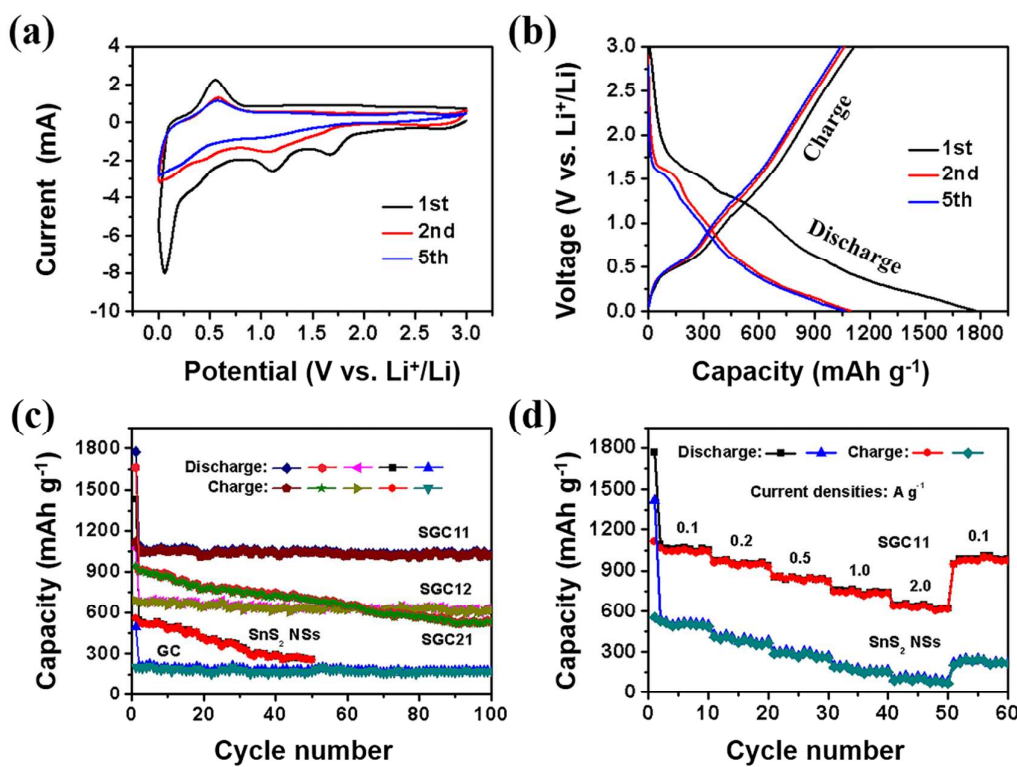


Figure 8

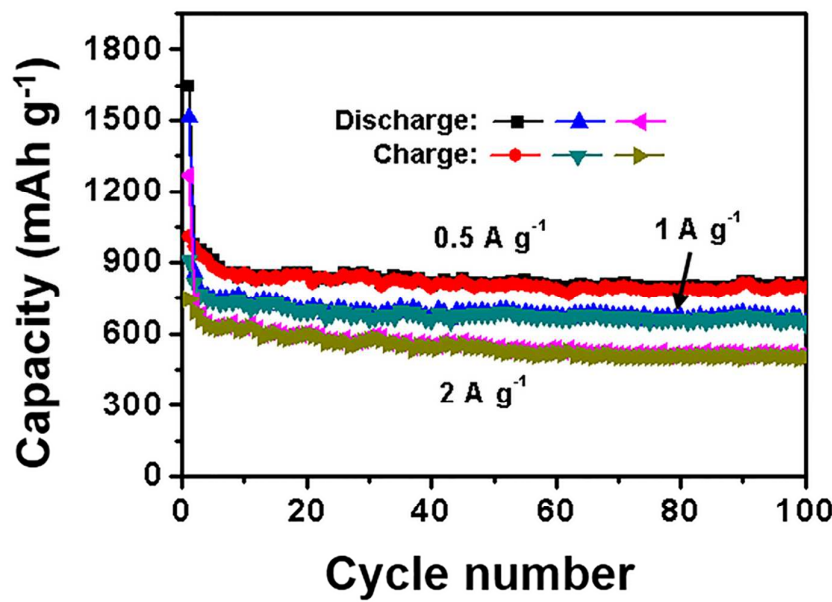


Figure 9

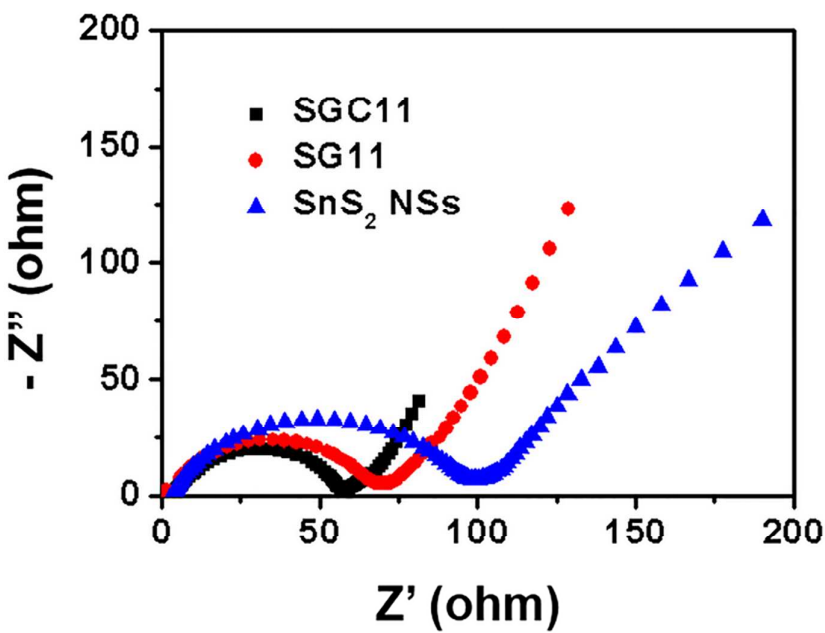


Figure 10

1
2
3
4 Graphic for the Table of Contents (TOC):
5
6

